Available online at www.sciencedirect.com
SCIENCE DIRECT®
Journal of Power Sources 119–121 (2003) 838–843
JOURNAL OF POWER SOURCES
www.elsevier.com/locate/jpowsour

Modeling of lithium-ion batteries

John Newman*, Karen E. Thomas, Hooman Hafezi, Dean R. Wheeler

Energy and Environmental Technologies Division, Lawrence Berkeley National Laboratory, and Department of Chemical Engineering, University of California, Berkeley, CA 94720, USA

Abstract

After reviewing the basic modeling framework for simulating battery behavior, three examples relating to mass-transfer effects are presented. Side reactions at the lithium electrode can change the surface concentration of lithium ions, introducing error into measurements of the cell potential as a function of bulk electrolyte concentration (concentration-cell measurements). This error introduced by a continuous side reaction is carried over into calculations of the transference number from the galvanostatic polarization method. Concentration gradients formed during passage of current are associated with a heat-of-mixing effect, which is the cause of heat generation during relaxation after cessation of the current. Finally, molecular dynamics simulations show that the decrease in conductivity with increasing salt concentration in liquid carbonate electrolytes is caused by ion association.
© 2003 Published by Elsevier Science B.V.

Keywords: Lithium battery; Model; Transference number; Side reactions; Heat of mixing; Thermal model; Conductivity; Molecular dynamics; Diffusion coefficient

1. Overview of modeling batteries

There are several key aspects of lithium-ion batteries that must be considered in any model of their behavior. The electrodes are generally porous, and therefore the distribution of the reaction through the depth of the electrode must be considered. The active material is an insertion compound, in which the chemical potential and other thermodynamic properties may vary continuously with inserted lithium concentration, and solid-state diffusion of lithium through the active material must be considered. Finally, as in most batteries, the electrolyte is a concentrated, nonideal solution, and mass transport across the electrolyte has a significant effect on battery performance. The modeling examples given in this paper all relate to mass transport in the electrolyte and/or insertion electrode.

The basic modeling framework consists of porous electrode theory, concentrated solution theory, Ohm's law, kinetic relationships, and charge and material balances [1,2]. Porous electrode theory [3] treats the porous electrode as a superposition of active material, electrolyte, and filler, with each phase having its own volume fraction. The material balances are averaged about a volume small with respect to the overall dimensions of the electrode but large with respect to the pore dimensions. This allows one to treat electrochemical reaction as a homogeneous term, without having to worry about the exact shape of the electrode–electrolyte interface.

Concentrated solution theory provides the relationship between driving forces (such as gradients in chemical potential) and mass flux [4]. The flux equation is then used in a standard material balance to account for the transient change of concentration due to mass flux and reaction. A charge balance is also needed to keep track of how much current has passed from the electrode into the electrolyte. Ohm's law describes the potential drop across the electrode and also in the electrolyte. In the electrolyte, Ohm's law is modified to include the diffusion potential. Finally, the Butler–Volmer equation generally is used to relate the rate of electrochemical reaction to the difference in potential between the electrode and solution, using a rate constant (exchange current density) that depends on the composition of the electrode and the electrolyte.

The dependent variables of concentration, potential, reaction rate, and current density each appear in more than one governing equation, and therefore the coupled governing equations must be solved simultaneously. In addition, material properties often vary considerably with concentration. Therefore, battery simulation requires a numerical technique, such as the finite-difference technique BAND(j) [5], that can solve multiple coupled, nonlinear differential equations.

* Corresponding author. Tel.: +1-510-642-4063; fax: +1-510-642-4778.
E-mail address: newman@newman.cchem.berkeley.edu (J. Newman).

0378-7753/03/$ – see front matter © 2003 Published by Elsevier Science B.V.
doi:10.1016/S0378-7753(03)00282-9

As mentioned above, concentrated solution theory is used to provide the flux equations. The principles of irreversible thermodynamics state that the flux of one species is caused by gradients in the electrochemical potential μ_i of all species present. Thus, the flux of one species is inherently coupled to the fluxes of all other species present, as set forth in the Stefan–Maxwell equations:

$$c_i \nabla \mu_i = \sum_j \frac{c_i c_j}{c_T \mathscr{D}_{ij}} (v_j - v_i) \quad (1)$$

where c_i is concentration, $\mathscr{D}_{ij}$ the diffusion coefficients, v the velocity, i and j the species indices, and c_T is the total molar concentration. With the Onsager reciprocal relations, these principles yield $n(n-1)/2$ transport properties, where n is the number of species in solution.

For example, for a binary electrolyte (one salt in one solvent) there are three species (anion, cation, and solvent) and thus $3 \times 2/2 = 3$ phenomenological transport properties, $\mathscr{D}_{+0}$, $\mathscr{D}_{-0}$, and $\mathscr{D}_{+-}$. Combinations of the $\mathscr{D}_{ij}$'s are more readily measurable as the conductivity κ, salt diffusity D, and cationic transference number t_+^0. For a binary electrolyte, concentrated solution theory provides the following flux equation for the cation:

$$\boldsymbol{N}_+ = -\nu_+ D \left(1 - \frac{\mathrm{d}\ln c_0}{\mathrm{d}\ln c}\right) \nabla c + \frac{\boldsymbol{i} t_+^0}{z_+ F} + \nu_+ c v_0 \quad (2)$$

where $\boldsymbol{N}$ is the flux, ν_+ the number of moles of cation per mole of salt, $\boldsymbol{i}$ the current density in solution, z_+ the charge of the cation, and F is Faraday's constant. One can see that treatment of mass transport in a binary electrolyte rigorously using concentrated solution theory involves little added complexity over the often-used dilute solution theory. However, concentrated solution theory uses the correct number of independent transport properties, and includes the concentration dependence of those properties, while dilute solution theory does not.

In the following sections, we discuss three separate analyses of mass-transport-related effects in lithium batteries. The first section demonstrates how a continuous side reaction could cause error in measurements of the transference number. The second section discusses the heat effect associated with the formation and relaxation of concentration gradients. The third section presents the results of molecular dynamics simulations which give insight into the decrease in conductivity with increasing salt concentration in liquid carbonate electrolytes.

2. Effect of side reactions on measurement of transport properties in polymer electrolytes

Measurement of the transference number in polymer electrolytes is difficult because the polymer electrolytes are opaque and poorly conductive. The galvanostatic polarization technique [6,7] was developed in our research group to provide a simple yet rigorous method of obtaining transference numbers in nonideal polymeric electrolytes.

Measurements using this method for the electrolyte lithium bis(trifluoromethylsulfonyl) (LiTFSI) in oxymethylene-linked poly(ethylene oxide) (PEMO), gave negative t_+^0 at low LiTFSI concentrations [8]. To check the validity of these measurements, simulations, using the measured transport properties, of transition times were compared to experimental transition-time data [9]. In a transition-time experiment, a high galvanostatic current is passed across a cell comprised of two lithium electrodes separated by the polymer electrolyte. If the current is above the limiting current, then eventually the salt concentration will be driven to zero at the cathode, causing the cell potential to rise rapidly. The time at which the potential rises rapidly is called the transition time. While the simulations closely matched the experimental transition times at moderate and high salt concentrations, there was a significant discrepancy at low salt concentrations. In addition, at low salt concentrations the experimental potential would bend over rather than shooting straight up (see Fig. 1). Such behavior is indicative of a side reaction consuming the current.

Other studies [10,11] have indicated that the solid-electrolyte interphase (SEI) formed on lithium in electrolytes containing LiTFSI salt is not a perfect barrier, and a continuous side reaction may occur through the SEI. Therefore, we investigated whether a continuous corrosive side reaction on the lithium metal could be introducing error into the measurement of t_+^0. The model side reaction is

$$\mathrm{S} + \mathrm{Li} \rightarrow \mathrm{S}^- + \mathrm{Li}^+ \quad (3)$$

where S represents the polymer (solvent) and S^- is the product of the side reaction.

The galvanostatic polarization method consists of four separate experiments, ac impedance to obtain κ, restricted diffusion to obtain D, and galvanostatic polarization and concentration-cell measurements which together, using the measured D, yield t_+^0 and the activity coefficient. Our analysis shows that a side reaction would have the largest effect on concentration-cell measurements, as described next.

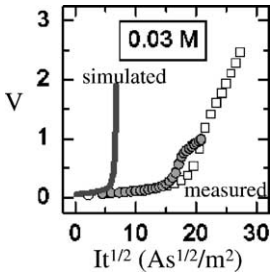

Fig. 1. Experimental (symbols) and simulated (solid line) cell potential as a function of time during galvanostatic current for 0.03 M LiTFSI in PEMO at 85 °C. The simulation, which has no side reaction, shows the potential rising steeply, whereas the bend in the experimental potential indicates a side reaction is present.

In a concentration-cell measurement, polymer-electrolyte films are made with different salt concentrations c_∞. A cell is then assembled consisting of Li|polymer (c_∞)|polymer (c_{ref})|Li. The potential of the cell U, which depends on the surface concentration of lithium ions, is then measured, for different values of c_∞. The slope of U plotted against $\ln c$ is used to calculate t_+^0 from galvanostatic polarization experiments [6]. However, if a side reaction changes the actual concentration of lithium ions adjacent to the surface of the lithium metal, then error is introduced into the slope of U versus the logarithm of the bulk concentration. The degree of error depends primarily on how thermodynamically favorable the side reaction is; i.e. how much the potential of the side reaction differs from the potential of lithium deposition. The relative error will be larger for smaller salt concentrations.

Fig. 2 shows the simulated effect of a side reaction on measurement of the transference number. A constant value of 0.5 (''true'' value, solid line) was input to the simulation. The effect of a side reaction on concentration-cell measurements for an ideal solution (for the case of $D_{\text{LiS}} = D_{\text{LiTFSI}}$) was simulated, and the simulated $\mathrm{d}U/\mathrm{d}\ln c$ was used to calculate the ''measured'' transference number based upon data from a simulated galvanostatic-polarization experiment [9]. Results are plotted versus c_∞/C^*, where $C^* = \sqrt{k_{\text{s,c}}k_{\text{m,a}}/k_{\text{m,c}}k_{\text{s,a}}}$, where the k's are the rate constants and s, m, c, and a specify side, main, cathodic, and anodic, respectively. As shown in Fig. 2, the ''measured'' transference number (dashed line) has significant error at low concentrations (indicated by the difference between the ''measured'' and the ''true'' values).

These results indicate that, if a side reaction (or other phenomenon such as a film of sparingly soluble salt) is increasing the surface lithium-ion concentration, then the measured t_+^0 will be lower than the true value at low salt concentrations. It should also be noted that the side reactions of concern here are those with relatively slow kinetics compared to the main reaction. Fast side reactions would be easily observable during any part of the galvanostatic polarization method, and our data do not indicate a fast side reaction. For slow side reactions, transition-time experiments provide a unique means of detecting the presence of the side reaction in addition to serving as a check on the validity of measured transport properties. One should note, however, that in many electrolytes the SEI does provide stable protection against side reactions. In these cases, the galvanostatic polarization method will yield accurate results.

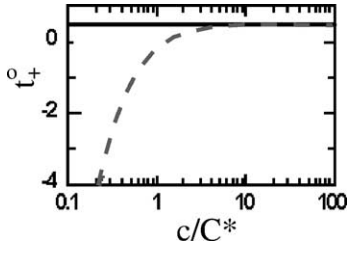

Fig. 2. Simulated effect of a side reaction on the measured t_+^0 (dashed line) obtained from a simulated solution in which the true t_+^0 (solid line) was 0.5.

3. Heat released during relaxation

The concentration gradients formed during passage of current also are associated with heat effects. This heat is that which is released (or possibly even absorbed) during relaxation after the current is turned off. An equal and opposite amount of heat is absorbed (or possibly released) during formation of the concentration gradients while current is flowing. This heat of relaxation is termed heat of mixing. An energy balance which includes the heat effects of heat of mixing is [12,13]

$$\dot{Q} = I\left(V - U^{\text{avg}} + T\frac{\partial U^{\text{avg}}}{\partial T}\right) + C_p\frac{\mathrm{d}T}{\mathrm{d}t} + \int\sum_i (\bar{H}_i - \bar{H}_i^{\text{avg}})\frac{\partial c_i}{\partial t}\,\mathrm{d}v \tag{4}$$

where $\dot{Q}$ is the rate of heat exchange with the surroundings, I the current (positive on discharge), V the cell potential, U the open-circuit potential, the superscript avg means evaluated at the volume-average concentration (e.g. U^{avg} is the potential to which the cell would relax if the current were interrupted), T the temperature, C_p the heat capacity, $\bar{H}_i$ the partial molar enthalpy of species i, and c is concentration. The first line is the standard energy balance used in the literature, which, while it does conserve energy, neglects the heat effects associated with heat of mixing, given in the term on the second line. This term is integrated over the total volume of the cell, including both the insertion electrodes and the electrolyte. If the partial molar enthalpies are constant with composition, then the heat of mixing term is zero.

Table 1 shows the magnitude of heat of mixing, calculated as the total amount of heat that would be released during relaxation after a $C/3$-rate discharge. Calculations are shown for two systems, Li|LiTFSI-PEMO|LiV_6O_{13} at 85 °C and Li|$LiPF_6$ in EC:DMC|$LiAl_{0.2}Mn_{1.8}O_{4-\delta}F_{0.2}$ at 25 °C. Parameters used in the simulations are given in [13–15]. For comparison, the total irreversible and entropic heat generated during the $C/3$-rate discharge is also shown.

Table 1
Magnitude of heat effects during a 3 h discharge in liquid-electrolyte and polymer-electrolyte cells

	ΔH (J/m^2)	
	Liquid	Polymer
Mixing in electrolyte	2	−52
Mixing in insertion material	20–130	55
Irreversible + entropic	7520	20160

The heat released during relaxation is much smaller than the resistive and entropic heat. For cells properly designed to mitigate concentration overpotential, heat of mixing will be negligible. However, it is interesting to note the relative magnitude of heat of mixing in the electrolyte versus that in electrode. In estimating the heat release during relaxation, one should consider heat of mixing in the electrolyte as well as mixing across the insertion electrode and radially within the particles of insertion material. In addition, heat of mixing can be endothermic or exothermic, depending on how $\bar{H}$ varies with composition. Heat of mixing will be exothermic during relaxation if $\partial\bar{H}/\partial c$ is positive.

4. Molecular dynamics simulations of transport in liquid electrolytes

Transport of lithium ions in the electrolyte is governed by the pairwise diffusion coefficients between all the n species in solution. As discussed in Section 1, this means one must know $n(n-1)/2$ diffusion coefficients. In addition, the diffusion coefficients vary with concentration. Few data are available in the literature, and experimental determination of the full set of diffusion coefficients for multicomponent solutions is daunting. Moreover, existing correlation and prediction methods in many cases cannot provide satisfactory accuracy in treating the nonideal concentrated solutions found in lithium batteries. There is therefore a need for a method to predict diffusional properties for concentrated mixtures of an arbitrary number of components.

Molecular dynamics (MD) is a simulation technique in which assumed intermolecular potentials are used to calculate trajectories of a modestly-sized collection of molecules. From such trajectories desired physical properties can be calculated [16]. MD shows promise as a predictive tool for transport properties since unlike other methods it can explicitly account for molecular geometry, electrical charges and polarity, steric hindrance, and an arbitrary number of species. While many MD simulations have been performed for simple ion-water systems [17], we are not aware of any simulations of bulk diffusion in liquid mixtures apart from binary mixtures of Lennard–Jones fluids [18,19].

One method by which bulk diffusion coefficients can be calculated is to cause a simulation to mimic experiment. For instance, an external electric field applied to the molecules in the simulation will induce an ionic current which can be readily computed and averaged. From the current and field one can then obtain electrical conductivity. Because of the small spatial and temporal extent of the simulation, it is generally necessary to impose fields far in excess of those used experimentally, and so an extrapolation back to the zero-field limit is often performed. This method of imposing external forces and measuring the sytem's response is known as nonequilibrium molecular dynamics (NEMD) and has been used previously by others to obtain a range of transport properties [16,18].

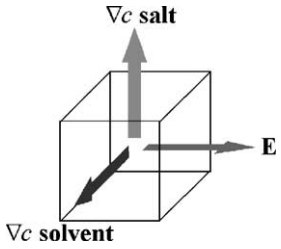

Fig. 3. Orthogonal external driving forces.

In the present work and for the first time, the NEMD method is extended to calculate the bulk diffusion matrix for a mixture containing more than two components. In addition, we effect a three-fold increase in efficiency through the use of multiple orthogonal external fields during a given simulation. Fig. 3 depicts how multiple orthogonal fields can act in concert to drive species diffusion in a way which mimics three simultaneous electrochemical experiments. In the simulations, external fields which mimic the effect of concentration gradients are used rather than actual concentration gradients. By using a scheme such as shown in Fig. 3 it is possible to extract a full set of diffusion coefficients for a mixture containing up to six species using only one simulation. Additional simulations would be required for $n > 6$.

We simulate two candidate electrolytes in this work: $LiPF_6$ in propylene carbonate (PC) and $LiPF_6$ in a 1:2 (w/w) mixture of ethylene carbonate (EC) and dimethyl carbonate (DMC).

MD requires the input of accurate intermolecular potentials to predict physical properties accurately. It is generally difficult to obtain accurate potentials, and in particular ones that also can be used for rapid computation. It is common, therefore, in MD simulations to use simplified pairwise potential forms which have only a few adjustable parameters. That approach is used here. Lennard–Jones centers and coulombic point charges are placed at atomic sites, that is, the locations of all atomic nuclei except for methyl groups, for which the group is treated as one site. The Lennard–Jones parameters and partial charges for all sites were initially taken from literature values [20], with some adjustment to improve the simulated densities of the pure solvents and the mixtures [21].

Each simulation included 450 molecules. Temperature and pressure during each simulation fluctuated, but were constrained to averages of 298 K and 0.1 MPa, respectively. Table 2 gives the NEMD results for diffusion coefficients

Table 2
Pairwise diffusion coefficients for 1 M $LiPF_6$ in PC and in 1:2 (w/w) EC/DMC

ab	PC	EC/DMC
$\mathscr{D}_{ab}$ (10^{-11} m^2/s)		
+0	1.9 (7.0)	3.5/9.0 (9.2/25.3)
−0	5.0 (17.1)	6.1/22.6 (24.1/31.1)
+−	0.2 (2.6)	0.2 (3.4)
00′	–	17.1

Experimental values given in parentheses.

of the two candidate electrolytes at 1 M $LiPF_6$ salt concentration, compared to experiment. There are three independent coefficients for the PC solvent (an $n = 3$ system), whereas there are six independent coefficients for the EC/DMC solvent (an $n = 4$ system). Interestingly, the interactions between the Li^+ cation and each of the EC/DMC co-solvents is different. Then a lithium-ion flux could cause a separation in the co-solvents across a battery separator. However, for a typical steady-state battery current of 1 mA/cm^2, the degree of separation will be less than 1% across a 25 μm-thick separator.

The experimental data for binary diffusivities presented in Table 2 are estimates based on conductivity and self-diffusion measurements of these systems or chemically similar ones [22–24], and so should be considered semi-quantitative only. Nevertheless, the simulations clearly underpredict the pairwise diffusivities, particularly between the two counterions. We believe that this discrepancy stems from overbinding between species, particularly the ions, due to the simplified intermolecular potentials.

Fig. 4 plots the viscosity and conductivity of the PC-based electrolyte versus salt concentration. The simulations consistently overpredict resistance to both mass and momentum transport, but in both cases reproduce the qualitative trend of the experimental data. This is encouraging; we believe that improvement in the accuracy of the intermolecular potentials will enable quantitative-level prediction of transport properties.

It has been stated in the literature [25] that the maximum in conductivity for electrolytes such as shown in Fig. 4 is caused by the increasing viscosity as salt concentration increases. Taking a molecular view, however, both macroscopic phenomena flow from molecular interactions. An examination of the 1 M $LiPF_6$ simulation shows that on average each ion is surrounded by 1.2 nearest neighbors of the oppositely charged counter-ion. These nearest neighbors are strongly bound, lying in a free-energy well of approximately $6kT$ depth. This means that most ions will be part of persistent neutral ion-pairs and will not contribute to conductivity. Ionic neighbors beyond this nearest shell do not experience this strong and persistent binding.

As the concentration is increased to 2.3 M $LiPF_6$, the simulations show each ion being surrounded by 2.2 strongly associated, oppositely charged nearest neighbors on average. This provides sufficient connectivity for ion chains and networks to form, which closely resemble the behavior of polymers in solution. This ionic aggregation would greatly diminish conductivity while at the same time causing a large increase in viscosity.

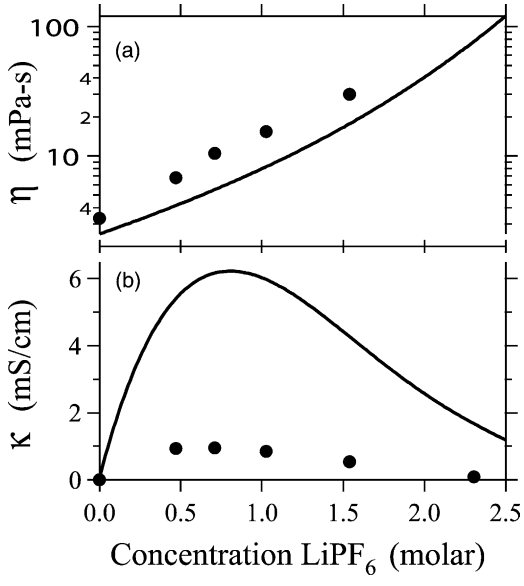

Fig. 4. Viscosity (a) and conductivity (b) of $LiPF_6$ in PC vs. concentration. Lines denote fits to experimental data [24], and points are simulation results.

Acknowledgements

This work was supported by the Assistant Secretary for Energy Efficiency and Renewable Energy, Office of Transportation Technologies, Electric and Hybrid Propulsion Division of the US Department of Energy under Contract #DE-AC0376SF00098.

References

[1] J. Newman, W. Tiedemann, Am. Inst. Chem. Eng. J. 21 (1975) 25.
[2] K.E. Thomas, R.M. Darling, J. Newman, Modeling of lithium batteries, in: Advances in Lithium-Ion Batteries, Kluwer Academic Publishers, New York, 2002.
[3] J. Newman, C.W. Tobias, J. Electrochem. Soc. 109 (1962) 1183.
[4] J.S. Newman, Electrochemical Systems, second ed., Prentice-Hall, Englewood Cliffs, NJ, 1991.
[5] J. Newman, I&EC Fundam. 7 (1968) 514.
[6] Y. Ma, M. Doyle, T.F. Fuller, M.M. Doeff, L.C. de Jonghe, J. Newman, J. Electrochem. Soc. 142 (1995) 1859.
[7] H. Hafezi, J. Newman, J. Electrochem. Soc. 147 (2000) 3036.
[8] H. Hafezi, S. Sloop, J. Kerr, J. Newman, in: Proceedings of the 198th Meeting of the Electrochemical Society, Phoeniz, Arizona, 22–27 October 2000 (abstract 155).
[9] H. Hafezi, Characterization of transport phenomena in polymer electrolyte systems, Ph.D. thesis, University of California, Berkeley, CA, 2002.
[10] D. Aurbach, E. Granot, Electrochim. Acta 42 (1997) 697.
[11] Y. Choquette, G. Brisard, M. Parent, J. Electrochem. Soc. 145 (1998) 3500.
[12] D. Bernardi, E. Pawlikowski, J. Newman, J. Electrochem. Soc. 132 (1985) 5.
[13] K.E. Thomas, Lithium-ion batteries: thermal and interfacial phenomena, Ph.D. thesis, University of California, Berkeley, CA, May 2002.
[14] K.E. Thomas, S.E. Sloop, J.B. Kerr, J. Newman, J. Power Sources 89 (2000) 132.
[15] K.E. Thomas, J. Newman, J. Electrochem. Soc. 150 (2003) A176.
[16] M. Allen, D. Tildesley, Computer Simulation of Liquids, Oxford Science, Oxford, 1989.
[17] S.-B. Zhu, S. Singh, G. Robinson, Modern nonlinear optics, in: Advances in Chemical Physics, Field-Perturbed Water, vol. 85, Wiley, New York, 1994, pp. 627–731.

[18] G. Morriss, D. Evans, Mol. Phys. 54 (1985) 629.
[19] M. Schoen, C. Hoheisel, Mol. Phys. 52 (1984) 33.
[20] A. Marquez, P.B. Balbuena, J. Electrochem. Soc. 148 (2001) A624–A635.
[21] D.R. Wheeler, J. Newman, 2002, in preparation.
[22] K. Hayamizu, Y. Aihara, S. Arai, C.G. Martinez, J. Phys. Chem. B 103 (1999) 519–524.
[23] J. Tarascon, D. Guyomard, Solid State Ionics 69 (1994) 293–305.
[24] K. Kondo, M. Sano, A. Hiwara, T. Omi, M. Fujita, A. Kuwae, M. Iida, K. Mogi, H. Yokoyama, J. Phys. Chem. B 104 (2000) 5040–5044.
[25] J.T. Dudley, D. Wilkinson, G. Thomas, R. LeVae, S. Woo, H. Blom, C. Horvath, M. Juzkow, B. Denis, P. Juric, P. Aghakian, J. Dahn, J. Power Sources 35 (1991) 59–82.